Theoretical study on the ground and excited states of the chromate anion CrO_4^{2-}

Shinya Jitsuhiro, Hiromi Nakai, Masahiko Hada, and Hiroshi Nakatsuji
Department of Synthetic Chemistry and Biological Chemistry, Faculty of Engineering, Kyoto University, Sakyou-ku, Kyoto 606-01, Japan and Institute for Fundamental Chemistry, 34-4, Tankano-Nishihiraki-cho, Sakyou-ku, Kyoto 606, Japan

(Received 12 July 1993; accepted 4 April 1994)

The symmetry adapted cluster (SAC) and SAC-configuration interaction (SAC-CI) theories are applied to the calculations of the ground and excited states of the chromate ion CrO_4^{2-}. Electron correlations are very large for this molecule and work to relax the charge polarization of the Cr–O bonds in the ground state. The experimental spectrum of CrO_4^{2-} is well reproduced by the present calculations, which is the first *ab initio* study of the excited states including electron correlations. All of the observed peaks are assigned to the dipole allowed transitions to the $^1T_2$ excited states. Furthermore, many kinds of forbidden transitions are calculated in the lower energy region. Both allowed and forbidden transitions are characterized as the electron-transfer excitations from oxygen to metal. In comparison with the previous theoretical studies, the present SAC-CI results are in good agreement with experiment and give reliable assignments of the spectrum. We also compare the electronic structures and spectra of CrO_4^{2-}, MoO_4^{2-}, MnO_4^-, RuO_4, and OsO_4, which have been studied by the SAC and SAC-CI methods.

I. INTRODUCTION

The chromate ion CrO_4^{2-}, which has been used extensively as an oxidizing agent, is isoelectronic with the permanganate ion MnO_4^-. The electronic structures of the ground and excited states of MnO_4^- have been studied experimentally.[1–3] On the theoretical side, several calculations have been carried out for spectral assignments.[4–8] The symmetry adapted cluster (SAC)[9] and SAC-configuration interaction (SAC-CI)[10] calculations gave reasonable assignments for the spectrum[8] and clarified the electronic mechanism of the photodissociation reaction of MnO_4^-.[11] Recently, a review article which explains the SAC/SAC-CI theory and its applications has been published.[12]

The electronic structures of the ground and excited states of CrO_4^{2-} have also been studied by many theoretical methods, since Teltow *et al.* reported the UV absorption spectrum of the ion in 1939.[13] In 1970, Johnson *et al.* observed the absorption spectrum of CrO_4^{2-} in the wide energy region.[14] The *ab initio* single excitation (SE)-CI calculations were carried out by Hiller *et al.*[5,6] for the spectral assignment of CrO_4^{2-}. Their assignment was limited to the lower energy region and their results did not agree well with the experimental values. On the other hand, some studies with the use of the $X\alpha$ method have been reported, namely, the MS-$X\alpha$ calculation by Gubanov *et al.*[15] and the $X\alpha$-SW one by Miller *et al.*[16]

In this study, we calculate the ground and excited states of CrO_4^{2-} by the SAC/SAC-CI method.[9,10,12] In particular, the usefulness of the SAC-CI method for the spectroscopic studies of the metal complexes has been confirmed by the applications to the complexes RuO_4, OsO_4, $MoO_{4-n}S_n^{2-}$ ($n=0$–4), $MoSe_4^{2-}$, $TiCl_4$, MnO_4^-, and CrO_2Cl_2.[8,17–20] We first investigate the electronic structure of the ground state, i.e., the bonding character between metal and ligands, the ionicity of the complex, etc. We next show the calculated excitation spectrum of the chromate ion and compare it with the experimental one. We give our assignment of the observed peaks in a wide energy region. We compare our results with the previous theoretical results. Furthermore, by comparing the present results for CrO_4^{2-} with the previous SAC-CI results for MoO_4^{2-}, MnO_4^-, RuO_4, and OsO_4, the similarity and difference in the electronic structures of the ground and excited states are clarified systematically. The concluding remarks are given in the last section.

II. COMPUTATIONAL DETAILS

The geometry of the CrO_4^{2-} ion is fixed to the regular tetrahedron with the metal–oxygen bond length of 1.675 Å, which is due to the experimental data.[21] The Gaussian basis sets used in this study are as follows: for the Cr atom, we use Huzinaga's $(14s8p5d)/[6s2p2d]$ set[22] augmented with the two p ($\zeta_p=0.109$, 0.036) functions[22] for representing the $4p$ orbital. For oxygen, we use the $(9s5p)/[4s2p]$ set of Huzinaga–Dunning.[23,24] The all-electron Hartree–Fock (HF) wave function for the ground state is calculated with the use of the program HONDO7.[25]

The electron correlations in the ground state are taken into account by the SAC theory[9] and those in the excited states by the SAC-CI theory[10] with the use of the program SAC85,[26] where the diagonalization part was modified for vectorization. The active space in the SAC/SAC-CI calculations involves 20 higher occupied orbitals and 36 lower unoccupied orbitals calculated by the HF method. The 20 occupied orbitals are mainly composed of the $3d$ atomic orbitals of Cr and the $2p$ atomic orbitals of O.

The SAC/SAC-CI calculations are performed in the C_{2v} subset of the T_d symmetry. The elements of the T_d symmetry t_1, t_2, e, a_1, and a_2 are connected with those of the C_{2v} symmetry as follows:

$$t_1=a_2+b_1+b_2, \quad t_2=a_1+b_1+b_2,$$

 0021-9606/94/101(2)/1029/8/$6.00

TABLE I. Dimensions of the SAC and SAC-CI calculations of CrO_4^{2-}.

Symmetry	After selection	Before selection
Ground state SAC		
$^1A_1$	3009	66 673
Excited state SAC-CI		
$^1A_1$	8440	66 673
$^1A_2$	7881	63 468
$^1B_1$	7909	64 980

$$e=a_1+a_2, \quad a_1=a_1, \quad a_2=a_2.$$

Since the B_1 and B_2 states are degenerate in this case, the calculation for the B_2 state was omitted.

In the SAC/SAC-CI calculations, all single-excitation operators included in the linked term and double excitation operators are selected by the second-order perturbation method.[27] For the ground state, the double-excitation operators whose perturbation energy contribution is larger than 1×10^{-4} hartree are included. For excited states, the threshold of 1×10^{-4} hartree is used with respect to the main configurations ($C\geqslant0.2$) of the 15 lower SE-CI solutions for each symmetry.

In the SAC theory, the effect of the simultaneous binary collisions (four-body collisions) of electrons is dealt with in the form of the unlinked term. We include in the unlinked term all the doubly excitation operators whose coefficients in the single and double-CI (SD-CI) are larger than 7×10^{-3}. In the SAC-CI theory, the transferable part of the electron correlation between the ground and excited states is expressed by the unlinked term. This term is expressed as the sum of double excitations from the main reference configurations of the state. These double excitations are those whose coefficients in the ground state SD-CI are larger than 1×10^{-3}, and the main reference configurations are selected as those whose coefficients in the SD-CI are larger than 1×10^{-1}.

Table I shows the dimensions of the SAC/SAC-CI calculations for the ground and excited states of CrO_4^{2-}. By virtue of the SAC/SAC-CI formalism, the dimensions of the calculations are small in comparison with those of the CI method of a comparable accuracy.

III. RESULTS AND DISCUSSIONS

A. Ground state

The self-consistent field (SCF) orbital sequence is shown in Table II, which involves only occupied valence and lower unoccupied orbitals up to the $4t_2$ molecular orbital (MO). Table II also shows the characters of the SCF orbitals; Cr(d) and O(p) denote the chromium d and oxygen p atomic orbitals (AOs), respectively, and Cr±O mean bonding (+) and antibonding (−) combinations. The lowest two valence orbitals $1t_2$ and $1e$ are the bonding MOs between the $3d$ orbitals of Cr and the $2p$ orbitals of O. The higher occupied orbitals $2t_2$, $1a_1$, and $1t_1$ are the nonbonding MOs composed mainly of the $2p$ orbitals of O. In particular, the highest occupied MO (HOMO) $1t_1$ is completely localized on oxygens. The sequence of the valence occupied MOs is the same as the Slater-type orbital (STO)-3G result of Hiller *et al.*,[5] though their larger basis set result is different in the ordering of the $2t_2$ and $1a_1$ MOs,[6] which are energetically close. However, the basic structure of the valence occupied MOs, i.e., two lower bonding MOs and three higher nonbonding MOs, is common in all the results. This is also common to the case of MnO_4^-.

TABLE II. Orbital energies and characters of the HF wave function for CrO_4^{2-}.

Symmetry	Character[a]	Orbital energy (eV)
Occupied orbitals		
$1t_2$	Cr($3d$)+O($2p$):B	−4.94
$1e$	Cr($3d$)+O($2p$):B	−4.31
$2t_2$	O($2p$):L	−2.16
$1a_1$	O($2p$):L	−1.96
$1t_1$	O($2p$):L	−0.78
Unoccupied orbitals		
$2a_1$	Cr($4s$):M	9.47
$3t_2$	Cr($4p$):M	10.77
$2e$	Cr($3d$)−O($2p$):A	12.37
$4t_2$	Cr($3d$)−O($2p$):A	12.98

[a]+ and − denote bonding and antibonding combinations, respectively. B, A, L, and M mean the boding, antibonding, ligand, and metal orbitals, respectively.

On the other hand, the sequence of the unoccupied orbitals is basis set dependent. In the present result, the lowest unoccupied MO (LUMO) is the $2a_1$ orbital, which consists mainly of the $4s$ orbital of Cr. The next LUMO is the $3t_2$ orbital, which consists mainly of the $4p$ orbitals of Cr and has a diffuse orbital character. The higher unoccupied orbitals $2e$ and $4t_2$ are the antibonding MOs between the $3d$ orbitals of Cr and the $2p$ orbitals of O.

Table III shows the total energies, the Mulliken atomic orbital populations, and the net charges of CrO_4^{2-} calculated by the HF and SAC methods. The correlation energy is −0.612 hartree by the SAC calculation. It is very large in comparison with the other systems.[8,17–20] While the formal charge of Cr in CrO_4^{2-} is +6, the Cr–O bond has large covalent character due to the back donation of electrons from O to Cr through the bonding MOs. The net charge of the Cr atom is +1.337 at the HF level and +1.122 at the SAC level. The ionicity of the Cr–O bond is relaxed by including electron correlations, which is common to all the metal complexes so far studied.

Table IV shows the occupation numbers of the natural orbitals of the SAC wave function. In comparison with the HF ones, the occupations of the $1t_1$ MOs decrease more than those of the other occupied MOs. In the unoccupied orbitals, the occupancies of the $3t_2$ and $2e$ MOs increase by including electron correlations. Needless to say that the natural orbitals themselves are different between the HF and SAC levels. These changes in the occupation numbers result in an increase of the $3d$ occupation of Cr and a decrease of the $2p$ occupation of O, as shown in Table III.

TABLE III. Total energy and the valence electron populations for the ground state of CrO_4^{2-} calculated by the HF and SAC methods.

Method	Energy (hartrees)	Cr				O		
		s	*p*	*d*	Charge	*s*	*p*	Charge
HF	−1 342.070 14	0.011	0.461	3.923	+1.337	1.937	4.903	−0.834
SAC	−1 342.681 96	0.048	0.505	4.120	+1.122	1.938	4.847	−0.780
Δ[a]	−0.611 82	+0.037	+0.044	+0.197	−0.215	+0.001	−0.056	+0.054

[a]The difference between HF and SAC values.

B. Excited states

Figure 1 shows the electronic spectra of the CrO_4^{2-} ion, the upper one being the experimental spectrum observed by Johnson *et al.*[14] and the lower one being the present theoretical spectrum calculated by the SAC/SAC-CI method. Table V shows the summary of the present SAC-CI results for the singlet excitation energy, main configuration, oscillator strength, and net charge of the excited state. While all the main configurations of the excited states are the single excitation configurations, the mixing of the configurations seems to increase as the excitation energy increases.

Almost all the main configurations of the excited states, whose excitation energies are from 2.95 to 6.05 eV, are the excitations from either of the $2t_2$, $1a_1$, and $1t_1$ MOs, which are the oxygen lone-pair MOs, to either of the $2e$, $4t_2$, $2a_1$, and $3t_2$ MOs, the former two being the Cr($3d$)–O($2p$) antibonding MOs and the latter two being the Cr $4s$ and $4p$ orbitals. The amplitudes in the unoccupied $2e$ and $4t_2$ MOs are larger at Cr than at O, and in particular, the $2e$ MO is mainly localized at Cr. Furthermore, the $2a_1$ and $3t_2$ MOs are localized on the Cr atom. Therefore, these transitions are all roughly characterized as the electron-transfer excitations from oxygen to metal, so that the ionic character of the Cr–O bond is relaxed in these excited states than in the ground state. Actually, the calculated net charge of the Cr atom, which is 1.12 for the ground state, is reduced to 0.8–0.5 and further to 0.4–0.16. In particular, this reduction is large for the transitions to the $2a_1$ and $3t_2$ MOs, as expected.

On the other hand, the excited states lying in the energy region 6.24–6.49 eV are the transitions from the $1t_2$ and $1e$ MOs, which are the Cr–O bonding MOs, to the $2e$ MO which is the Cr–O antibonding MO. Therefore, the Cr net charge is relatively large (0.85–0.95) in comparison with the lower states described above. Our calculated highest state $8\,^1T_2$ has the same character as the lower excited states, i.e., ligand to metal charge transfer excitation, and therefore the

TABLE IV. Occupation number of the HF orbital and the SAC natural orbital for the ground state of CrO_4^{2-}.

Orbital	HF	SAC	Difference
Occupied manifold			
$1t_2$	6.0	5.9456	−0.0544
$1e$	4.0	3.9346	−0.0654
$2t_2$	6.0	5.9191	−0.0809
$1a_1$	2.0	1.9748	−0.0282
$1t_1$	6.0	5.8687	−0.1313
Unoccupied manifold			
$2a_1$	0.0	0.0069	+0.0069
$3t_2$	0.0	0.1841	+0.1841
$2e$	0.0	0.1032	+0.1032
$4t_2$	0.0	0.0251	+0.0251

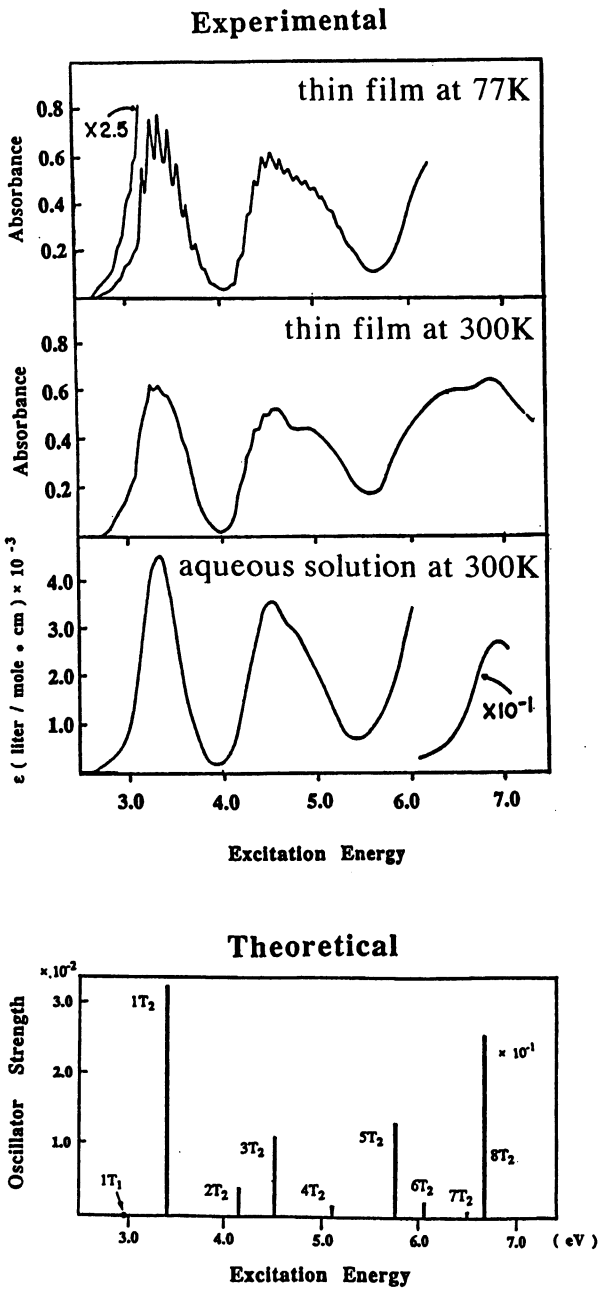

FIG. 1. Experimental and theoretical electronic excitation spectra of CrO_4^{2-}.

TABLE V. Summary for the ground and excited states of CrO_4^{2-}.

State	SAC/SAC-CI					Experimental[a]	
	Main configuration[b]	Excitation energy (eV)	Oscillator strength[c]	Net charge		Excitation energy (eV)	Oscillator strength
				Cr	O		
XA_1	HF	0.00	···	+1.122	−0.780	···	···
$1T_1$	$0.95(1t_1\rightarrow 2e):L\rightarrow A$	2.95	Forbidden	+0.753	−0.642	2.95	
$1T_2$	$0.90(1t_1\rightarrow 2e):L\rightarrow A$	3.41	0.0317	+0.762	−0.691	3.38	*S*
$2T_1$	$0.91(1t_1\rightarrow 2a_1):L\rightarrow A$	3.89	Forbidden	+0.161	−0.540		
$1E$	$0.67(1t_1\rightarrow 4t_2):L\rightarrow A$ $0.66(1t_1\rightarrow 3t_2):L\rightarrow M$	4.10	Forbidden	+0.680	−0.670		
$3T_1$	$0.79(2t_2\rightarrow 2e):L\rightarrow A$	4.15	Forbidden	+0.674	−0.669		
$2T_2$	$0.70(1t_1\rightarrow 3t_2):L\rightarrow M$ $0.59(1t_1\rightarrow 4t_2):L\rightarrow A$	4.16	0.0033	+0.615	−0.654		
$3T_2$	$0.88(2t_2\rightarrow 2e):L\rightarrow A$	4.51	0.0108	+0.817	−0.704	4.56	*S*
$4T_1$	$0.62(1t_1\rightarrow 3t_2):L\rightarrow M$ $0.51(2t_2\rightarrow 2e):L\rightarrow A$ $0.46(1t_1\rightarrow 4t_2):L\rightarrow A$	4.58	Forbidden	+0.625	−0.656		
$1A_2$	$0.75(1t_1\rightarrow 3t_2):L\rightarrow M$ $0.58(1t_1\rightarrow 4t_2):L\rightarrow A$	4.58	Forbidden	+0.548	−0.637		
$2E$	$0.95(1a_1\rightarrow 2e):L\rightarrow A$	4.63	Forbidden	+0.790	−0.698		
$4T_2$	$0.74(2t_2\rightarrow 2a_1):L\rightarrow M$	5.11	0.0008	+0.344	−0.586		
$2A_1$	$0.63(2t_2\rightarrow 3t_2):L\rightarrow M$ $0.47(1a_1\rightarrow 2a_1):L\rightarrow M$ $0.47(2t_2\rightarrow 4t_2):L\rightarrow A$	5.46	Forbidden	+0.413	−0.603		
$3E$	$0.65(1t_1\rightarrow 3t_2):L\rightarrow M$ $0.51(1t_1\rightarrow 4t_2):L\rightarrow A$	5.53	Forbidden	+0.535	−0.634		
$5T_1$	$0.64(2t_2\rightarrow 4t_2):L\rightarrow A$ $0.51(2t_2\rightarrow 3t_2):L\rightarrow M$	5.68	Forbidden	+0.695	−0.674		
$5T_2$	$0.52(2t_2\rightarrow 2a_1):L\rightarrow M$ $0.47(1t_1\rightarrow 3t_2):L\rightarrow M$ $0.44(2t_2\rightarrow 3t_2):L\rightarrow M$	5.74	0.0138	+0.364	−0.591		
$2A_2$	$0.57(1t_1\rightarrow 4t_2):L\rightarrow A$ $0.51(1t_1\rightarrow 3t_2):L\rightarrow M$ $0.45(1e\rightarrow 2e):B\rightarrow A$	5.77	Forbidden	+0.566	−0.642		
$3A_1$	$0.80(1a_1\rightarrow 2a_1):L\rightarrow M$ $0.45(2t_2\rightarrow 4t_2):L\rightarrow A$	5.77	Forbidden	+0.606	−0.651		
$6T_1$	$0.58(1t_1\rightarrow 4t_2):L\rightarrow A$ $0.56(1t_1\rightarrow 3t_2):L\rightarrow M$ $0.45(1t_2\rightarrow 2e):B\rightarrow A$	5.79	Forbidden	+0.545	−0.636		
$4A_1$	$0.63(2t_2\rightarrow 3t_2):L\rightarrow M$ $0.45(2t_2\rightarrow 4t_2):L\rightarrow A$ $0.40(1t_1\rightarrow 4t_2):L\rightarrow A$	5.81	Forbidden	+0.417	−0.604		
$3A_2$	$0.54(2t_2\rightarrow 3t_2):L\rightarrow M$ $0.53(1t_1\rightarrow 4t_2):L\rightarrow A$	5.82	Forbidden	+0.634	−0.658		
$6T_2$	$0.47(2t_2\rightarrow 3t_2):L\rightarrow M$ $0.40(1t_1\rightarrow 4t_2):L\rightarrow A$	6.05	0.0016	+0.566	−0.642	6.20	*W*
$7T_1$	$0.69(1t_2\rightarrow 2e):B\rightarrow A$ $0.40(1t_1\rightarrow 4t_2):L\rightarrow A$	6.24	Forbidden	+0.852	−0.713		
$4A_2$	$0.85(1e\rightarrow 2e):B\rightarrow A$	6.32	Forbidden	+0.911	−0.728		
$4E$	$0.89(1e\rightarrow 2e):B\rightarrow A$	6.34	Forbidden	+0.921	−0.730		
$7T_2$	$0.82(1t_2\rightarrow 2e):B\rightarrow A$	6.49	0.0004	+0.942	−0.736		
$8T_2$	$0.60(1a_1\rightarrow 3t_2):L\rightarrow M$ $0.58(2t_2\rightarrow 3t_2):L\rightarrow M$	6.63	0.2518	+0.326	−0.582	6.89	*S*

[a]Reference 14.
[b]*B*, *A*, *L*, and *M* means the bonding, antibonding, ligand, and metal orbitals, respectively.
[c]The transition to the T_2 state is symmetry allowed.

charge polarization is much reduced in this state.

In the T_d symmetry, only the transitions to the singlet T_2 states are dipole allowed. We assign the observed bands to the allowed transitions to the $^1T_2$ states. The calculated lowest excited state is the symmetry-forbidden $1\,^1T_1$ state, which has the main configuration of the excitation from $1t_1$ to $2e$, and the calculated excitation energy is 2.95 eV. All the lowest excited states of the complexes MnO_4^-,[8] OsO_4, RuO_4,[17] $TiCl_4$,[19] and CrO_2Cl_2 (Ref. 20) calculated by the SAC/SAC-CI method have the same excitation character. While this transition is dipole forbidden, a weak shoulder corresponding to this state is found at 2.95 eV on the left-hand side of the first strong band of the experimental spectrum shown in Fig. 1. Since this state is located close to the

dipole-allowed transition, i.e., $1\ ^1T_2$ as discussed below, it is able to gain intensity through the vibronic coupling.

The first strong peak observed at 3.38 eV is assigned to the allowed transition to the $1\ ^1T_2$ state calculated at 3.41 eV. The oscillator strength is calculated to be 0.0317, which is relatively large among the calculated values. Duinker *et al.*[28] observed the electronic spectrum of K_2CrO_4 in the K_2SO_4 crystal, which has a C_s symmetry, and showed the splitting of this peak into three parts. This fact corresponds to the present assignment of the first peak to the triply degenerate $1\ ^1T_2$ state. For the lowest two states ($1\ ^1T_1$ and $1\ ^1T_2$ states), the transitions are from the nonbonding orbital of O to the antibonding orbital between Cr and O, and therefore the force constant should be smaller in the excited states than in the ground state.[14]

The second strong band observed at 4.56 eV is assigned to the transition to the $3\ ^1T_2$ state calculated at 4.51 eV. The calculated oscillator strength is 0.0108. The excitation nature is similar to that of the first peak and in accord with the result of the vibrational analysis experiment.[14] The second band has a shoulder at about 5 eV in the higher energy region. Johnson *et al.* assigned this shoulder to the $1t_1 \rightarrow 3t_2$ transition.[20] In the present calculation, this is the main configuration of the $2\ ^1T_2$ state calculated at 4.16 eV with the small oscillator strength of 0.0033. It lies in the lower energy region. In the present calculation, we assign this shoulder peak to the transition to the $4\ ^1T_2$ state, whose main configuration is $2t_2 \rightarrow 2a_1$. The calculated excitation energy is 5.11 eV and the oscillator strength is 0.0008, which is small.

In the experimental spectra of CrO_4^{2-} shown in Fig. 1, there seems to be no shoulder peak in the lower-energy region of the second strong band. However, in the experimental spectrum for MnO_4^-, an isoelectronic molecule, there is a shoulder peak in the lower-energy side of the second strong band.[2] The CI calculations of Dahl and Johansen[29] and our SAC-CI calculations[8] for the MnO_4^- ion showed that the peak is originated from the $2\ ^1T_2$ ($1t_1 \rightarrow 3t_2$) state. It would be worthwhile to investigate the existence of the shoulder peak at ~4.16 eV by performing more accurate experiments for the excited states of CrO_4^{2-}.

In the experimental spectrum, a shoulder band is observed at the lower-energy region of the third strong band. This shoulder peak may be assigned either to the $5\ ^1T_2$ state calculated at 5.74 eV, or to the $6\ ^1T_2$ state calculated at 6.05 eV. The former assignment has a difficulty in that the calculated energy is too small and the latter one in that the calculated intensity is too small. Both excitations have mixed main configurations, but commonly have the $2t_2 \rightarrow 3t_2$ transition as a component. In the spectrum of MnO_4^-, there is a similar peak at 5.45 eV and the SAC-CI study[8] assigned it to the state represented by the mixed configurations $2t_2 \rightarrow 3t_2$ and $1a_1 \rightarrow 3t_2$. For the final assignment of this shoulder peak of CrO_4^{2-}, more detailed study seems to be necessary.

A very strong peak observed at 6.89 eV is the most characteristic absorption band of the CrO_4^{2-} ion. In the present calculation, it is assigned to the $8\ ^1T_2$ state calculated at 6.63 eV. The main configurations are represented by the $1a_1 \rightarrow 3t_2$ and $2t_2 \rightarrow 3t_2$ excitations, which are the ligand to metal charge transfer transitions. The ionicity of the Cr–O bond is most relaxed in this state among the calculated symmetry-allowed $^1T_2$ states. The Cr net charge is as small as +0.326. In agreement with this observation, the calculated oscillator strength is as large as 0.2518 and this is in accord with the experimental trend. The $7\ ^1T_2$ state calculated at the lower energy side (6.49 eV) with a small intensity (0.0004) may also constitute this strong band.

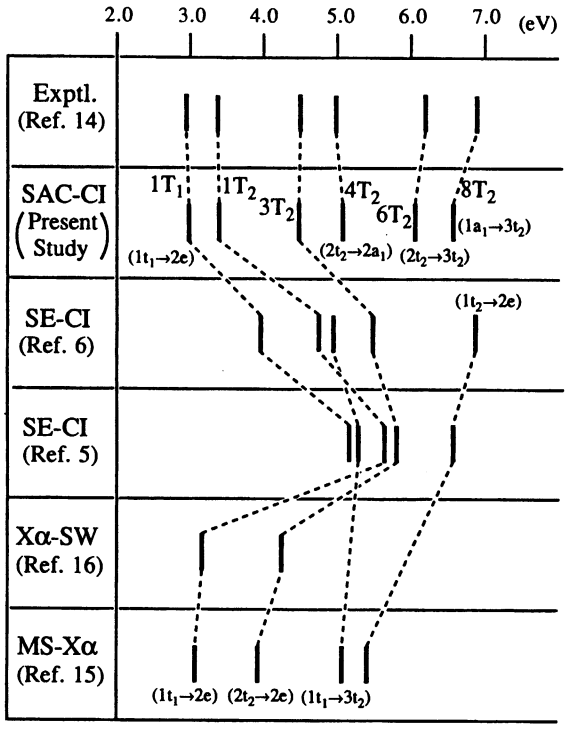

FIG. 2. A comparison of the different theoretical assignments of the observed excitation spectrum of CrO_4^{2-}.

As seen in Fig. 1, the intensity of this absorption band decreases very much when we use the Cs_2CrO_4 film instead of the solution. As a reason, it was thought that this excited state may have a diffuse nature and it is much influenced by the surrounding conditions. Actually, in the present calculations, the $3t_2$ orbital has a large contribution of the diffuse p orbitals. Theoretical study on the effect of the surrounding materials on the $3t_2$ orbitals of CrO_4^{2-} is interesting.

Finally, we compare the present SAC-CI results with the results of the previous calculations by the SE-CI,[5,6] $X\alpha$-SW,[16] and MS-$X\alpha$[15] methods. Figure 2 shows the comparison. Among the theoretical results so far obtained, the SAC-CI result shows best overall agreement with the experimental peaks. The earlier SE-CI results of Hiller and Saunders are too high in energy and are strongly basis-set dependent, while these studies certainly have historical values.[10,11] In the $X\alpha$-SW and MS-$X\alpha$ studies, the first strong peak is reasonably calculated as the present result, but the second peak is calculated at rather too low energy. The most prominent peak of CrO_4^{2-} at about 6.9 eV is not well reproduced by these calculations except for the SAC-CI one.

TABLE VI. Exciation energies (in electron volts), oscillator strengths, and main configurations for the lowest three $^1T_2$ states of CrO_4^{2-}, MoO_4^{2-}, MnO_4^-, RuO_4, and OsO_4.

		SAC/SAC-CI			Experimental	
Complex	State	Main configuration[a]	Excitation energy[b]	Oscillator strength	Excitation energy	Intensity
CrO_4^{2-}	$1\,^1T_2$	$1t_1 \rightarrow 2e:L \rightarrow A$	3.41(+0.03)	0.0317	3.38	*S*
	$2\,^1T_2$	$1t_1 \rightarrow 3t_2:L \rightarrow M$	4.16	0.0033		
	$3\,^1T_2$	$2t_2 \rightarrow 2e:L \rightarrow A$	4.51(−0.05)	0.0108	4.56	*S*
MoO_4^{2-}	$1\,^1T_2$	$1t_1 \rightarrow 3t_2:L \rightarrow M$	4.37	0.000		
	$2\,^1T_2$	$2t_2 \rightarrow 3t_2:L \rightarrow M$	5.14(−0.22)	0.049	5.36	*S*
	$3\,^1T_2$	$1t_1 \rightarrow 2e:L \rightarrow A$	5.52	0.026		
MnO_4^-	$1\,^1T_2$	$1t_1 \rightarrow 2e:L \rightarrow A$	2.57(+0.30)	0.0202	2.27	*S*
	$2\,^1T_2$	$1t_1 \rightarrow 3t_2:L \rightarrow A$	3.58(+0.11)	0.0045	3.47	*W*
	$3\,^1T_2$	$2t_2 \rightarrow 2e:L \rightarrow A$	3.72(−0.27)	0.0136	3.99	*S*
RuO_4	$1\,^1T_2$	$1t_1 \rightarrow 2e:L \rightarrow A$	3.22(0.00)	0.0128	3.22	*S*
	$2\,^1T_2$	$2t_2 \rightarrow 2e:L \rightarrow A$	4.55(+0.46)	0.0058	4.09	*S*
	$3\,^1T_2$	$1t_1 \rightarrow 3t_2:L \rightarrow A$	5.23(+0.20)	0.0001	5.03	*W*
OsO_4	$1\,^1T_2$	$1t_1 \rightarrow 2e:L \rightarrow A$	3.90(−0.44)	0.0365	4.34	*S*
	$2\,^1T_2$	$2t_2 \rightarrow 2e:L \rightarrow A$	5.46(+0.46)	0.0782	5.21	*S*
	$3\,^1T_2$	$1t_1 \rightarrow 3t_2:L \rightarrow A$	6.41(+0.46)	0.0221	5.95	*W*
Average discrepancy			0.25			

[a] *L*, *M*, and *A* mean the ligand, metal, and antibonding MOs, respectively.
[b] Values in parentheses show the difference from the experimental values.

C. A comparison with other tetraoxo metal complexes

In this section, we compare the electronic structure and property of CrO_4^{2-} with those of MoO_4^{2-}, MnO_4^-, RuO_4, and OsO_4, which have been studied by the SAC/SAC-CI calculations in our laboratory.[8,17,18] The central metals of these tetraoxo complexes belong to the groups VI, VII, and VIII in the Periodic Table.

PERIODS \ GROUPS	VI	VII	VIII
4	Cr	Mn	
5	Mo		Ru
6			Os

The numbers of their valence electrons are equal, while the oxidation numbers of the metals are +VI, +VII, and +VIII.

The colors of the CrO_4^{2-}, MnO_4^-, and RuO_4 solutions are yellow, purple, and orange, respectively, while both MoO_4^{2-} and OsO_4 are colorless. These differences are due mainly to the positions of the first absorption bands, which correspond to the allowed excitations to the $1\,^1T_2$ states. Table VI shows the excitation energies, the oscillator strengths, and the main configurations of the lowest three $^1T_2$ states, which are symmetry allowed, calculated by the SAC/SAC-CI method. In Table VI, the positions and the intensities of the band maxima in the experimental absorption spectra are also shown, which are due to the assignments of the previous and the present SAC/SAC-CI studies, and the differences between the calculated and the experimental excitation energies are shown in parentheses. Since the average discrepancy is 0.25 eV and the calculated oscillator strengths compare well with the experimental spectra, we can say again that these SAC/SAC-CI assignments are quite reliable. We note that the agreement with the experiment is improved as the calculation has been done more recently because the improvements not only in the computational facilities, but also in the calculational algorithms have allowed us to use better basis set and larger active space.

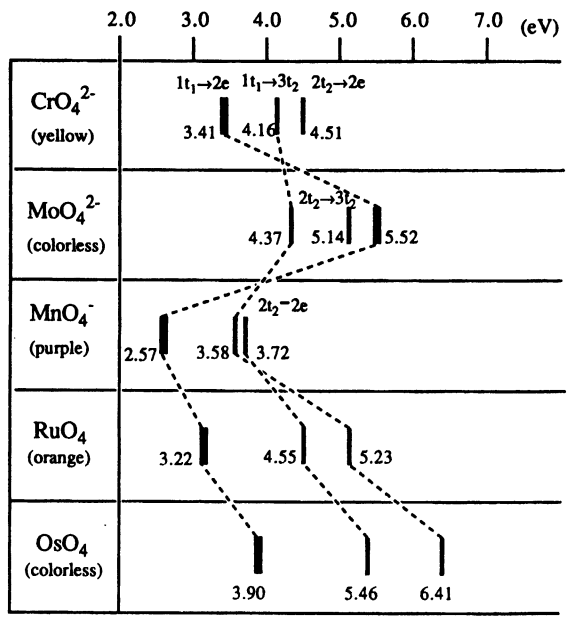

FIG. 3. A comparison of the calculated excitation energies for the lowest three $^1T_2$ states of CrO_4^{2-}, MoO_4^{2-}, MnO_4^-, RuO_4, and OsO_4.

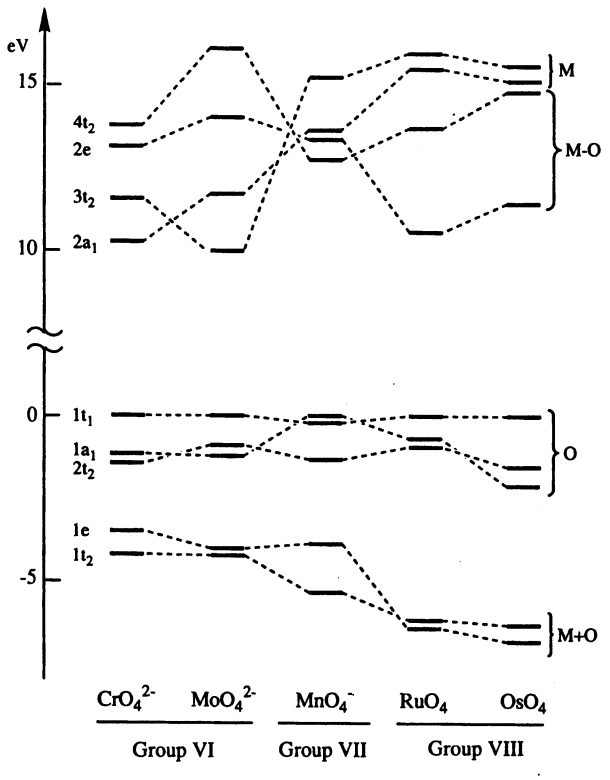

FIG. 4. Orbital energy levels of CrO_4^{2-}, MoO_4^{2-}, MnO_4^-, RuO_4, and OsO_4. The values are shown by electron volts with respect to the HOMOs as the reference levels. The MOs having the same character are connected by the dotted line.

Figure 3 shows the comparison of the excitation energies and the excitation natures for the lowest three $^1T_2$ states. Except for MoO_4^{2-}, all the main configurations of the $1\,^1T_2$ states are the single excitations from $1t_1$ to $2e$. The main configurations of the $1\,^1T_2$ and $3\,^1T_2$ states of MoO_4^{2-} are $1t_1 \rightarrow 3t_2$ and $1t_1 \rightarrow 2e$ transitions, respectively. Only MnO_4^- has the band maximum of the $1\,^1T_2$ state in the visible region of 1.6–2.9 eV. The complementary color of green, which corresponds to the absorption of photon energy 2.27 eV, is purple, which agrees with the color of MnO_4^-. The photon energies of the complementary colors of yellow and orange are about 2.6 and 2.5 eV, respectively. Since the first band maxima of CrO_4^{2-} and RuO_4 are 3.38 and 3.22 eV, respectively, which are in the UV region, the tails in lower visible energy region of these bands are important for the colors of the complexes.

Roughly speaking, the excitation energy E_{ia} of the transition from the ith MO ϕ_i to the ath MO ϕ_a is approximately represented by

$$E_{ia} = -\epsilon_i + \epsilon_a - J_{ia} + 2K_{ia} = \Delta\epsilon_{ia} - J_{ia} + 2K_{ia}, \qquad (1)$$

where ϵ is orbital energy, and J and K are Coulomb and exchange integrals, respectively. K_{ia} is sufficiently smaller than J_{ia}. J_{ia} becomes smaller with increasing the distance between the centers of the electron densities of ϕ_i and ϕ_a.

Figure 4 shows the orbital energy levels of the valence occupied and lower unoccupied MOs. We show the comparative energy levels with respect to the HOMOs, since the absolute orbital energies are quite different due to the difference in charge of the complexes. The orbital energies of the HOMOs of CrO_4^{2-}, MoO_4^{2-}, MnO_4^-, RuO_4, and OsO_4 are -0.78, -0.90, -7.68, -14.67, and -14.32 eV, respectively. For CrO_4^{2-}, the $(1t_2,1e)$, $(2t_2,1a_1,1t_1)$, $(2a_1,3t_2)$, and $(2e,4t_2)$ MOs have M(d)+O(p), O(p), M(s,p), and M(d)–O(p) characters, respectively, as mentioned before. In all these complexes, the occupied MOs have the same characters, and the MO levels of the M(d)+O(p) bonding characters are lower than those of the O(p) lone-pair one. On the other hand, the characters of $3t_2$ and $4t_2$ MOs are reversed for MnO_4^-, RuO_4, and OsO_4. It is also noted that the MO levels of the M(s,p) metal character are higher than those of the M(d)–O(p) antibonding one for the groups VII (Mn) and VIII (Ru, Os) metal complexes, while the reverse is true for the group VI (Cr, Mo) metal complexes.

This difference reflects in the excited state of the $1t_1 \rightarrow 3t_2$ transition. Namely, the $^1T_2$ $(1t_1 \rightarrow 3t_2)$ state is characterized by the excitation from O(p) to M(d)–O(p) in the group VII and VIII metal complexes, while it is characterized by the excitation from O(p) to M(p) in the group VI metal complexes. Furthermore, this state of MoO_4^{2-} is the first $^1T_2$ state, while those of the other complexes are the second or the third ones, as shown in Fig. 3.

Table VII shows the net charges for the ground states of the complexes obtained by the SAC calculations, which use the experimental bond lengths shown in Table VII. The negative charge of the oxygen decreases as the formal charge of the complex decreases, while the positive charges of the metals are not ordered.

In Fig. 3 and Table VI, we can find that the excitation energy to the $^1T_2$ state having the main configuration of

TABLE VII. The net charge and bond length for the ground state of the tetraoxo Cr, Mo, Mn, Ru, and Os complexes.

	Group VI		Group VII	Group VIII	
	CrO_4^{2-}	MoO_4^{2-}	MnO_4^-	RuO_4	OsO_4
Net charge					
M	+1.12	+1.28	+1.04	+1.44	+1.12
O	−0.78	−0.82	−0.51	−0.36	−0.28
Bond length (Å)	1.675	1.765	1.627	1.706	1.711

$1t_1 \rightarrow 2e$ decreases as the central metal atom shifts to the upper-right-hand side in the Periodic Table. Since the $1t_1$ and $2e$ MOs have M(d)–O(p) and O(p) natures, respectively, J_{ia} would become smaller as the bond length becomes longer and as the ligand $2e$ MO expands due to the negative charge. For the central metal on the upper-right-hand side in the Periodic Table, the orbital energy gap between the $1t_1$ and $2e$ MOs decreases as shown in Fig. 4, and the bond length and the net charge of O increases as shown in Table VII. In the case between CrO_4^{2-} and MnO_4^-, the value of J_{ia} is important for the excitation energy difference, since the orbital energy gap has reverse tendency, namely, 13.15 and 13.47 eV, respectively. By comparing between RuO_4 and OsO_4, the effect of the negative charge of O is understood to be smaller than those of the bond length and the orbital energy gap. Anyway, we must note that it is difficult to understand the SAC-CI results, including electron correlations which are essential, only through the crude approximation given by Eq. (1).

IV. CONCLUDING REMARKS

We have applied the SAC/SAC-CI method to the calculations of the ground and excited states of the chromate ion CrO_4^{2-}. We found that electron correlations are very important for the descriptions of the ground and excited states.

In contrast to the formal valence number of the Cr ion in this complex, the Cr–O bond is found to be much neutralized and have a large covalent character due to the back donation of electrons from O to Cr through the bonding MOs. Furthermore, the ionic character of the Cr–O bond is relaxed by including electron correlations

The theoretical excitation spectrum calculated by the SAC-CI method compares well with the experimental spectrum. All the observed peaks are assigned as being due to the dipole-allowed transitions to the $^1T_2$ states. The maximum discrepancy between the experimental and theoretical excitation energies is 0.26 eV. The present SAC-CI assignment differs from the previous ones as summarized in Fig. 2. The electronic transitions below 6 eV are characterized as the transitions from the nonbonding orbitals of the O ligands to the antibonding orbitals between Cr and O or to the localized orbitals on Cr, and some transitions have mixed nature. Therefore, along these transitions, electrons flow from the oxygens to the metal, greatly reducing the polarity of the Cr–O bonds.

The present study shows that electron correlations are quite important even for a qualitative assignment of the excitation spectrum of CrO_4^{2-}. The SE-CI results are unreliable as shown in Fig. 2, and most of the previous theoretical results are also unreliable, since they do not include a sufficient amount of electron correlations. We think that the present SAC-CI assignment is so far most reliable. We may safely conclude that the SAC-CI method is useful for studying the excited states of metal complexes, as has been shown for several metal complexes.[8,17–20]

Finally, by using the present and previous SAC/SAC-CI results for CrO_4^{2-}, MoO_4^{2-}, MnO_4, RuO_4, and OsO_4, we have discussed the similarity and difference in the electronic structures and spectra of these complexes.

ACKNOWLEDGMENTS

The calculations have been carried out with the use of the HITAC M-680H and S-820 computers at the Institute for Molecular Science. This study has been partially supported by the Grant-in-Aid for Scientific Research from the Japanese Ministry of Education, Science, and Culture. We acknowledge valuable comment of the referee on the comparison between CrO_4^{2-} and other tetraoxo metal complexes.

[1] J. Teltow, Z. Phys. Chem. B **40**, 397 (1938).
[2] L. Holt and C. J. Ballhausen, Theor. Chim. Acta. **7**, 313 (1967).
[3] L. W. Johnson and S. P. McGlynn, J. Chem. Phys. **55**, 2985 (1971); Chem. Phys. Lett. **10**, 595 (1971); L. W. Johnson, E. Hughes, and S. P. McGlynn, J. Chem. Phys. **55**, 4476 (1971).
[4] M. Wolfsberg and L. Helmholz, J. Chem. Phys. **20**, 837 (1952).
[5] I. H. Hillier and V. R. Saunders, Proc. R. Soc. London Ser. A **320**, 161 (1970).
[6] I. H. Hillier and V. R. Saunders, Chem. Phys. Lett. **9**, 219 (1971).
[7] H. Johansen, Chem. Phys. Lett. **17**, 569 (1972); H. Johansen and S. Rettrup, Chem. Phys. **74**, 77 (1983); H. Johansen, Mol. Phys. **49**, 1209 (1983).
[8] H. Nakai, Y. Ohmori, and H. Nakatsuji, J. Chem. Phys. **95**, 8287 (1991).
[9] H. Nakatsuji and K. Hirao, J. Chem. Phys. **68**, 2035 (1978).
[10] H. Nakatsuji, Chem. Phys. Lett. **59**, 362 (1978); **67**, 329 (1979); **67**, 334 (1979).
[11] H. Nakai and H. Nakatsuji, J. Mol. Structure (THEOCHEM) in press; H. Nakai, Y. Ohmori, and H. Nakatsuji (to be published).
[12] H. Nakatsuji, Acta. Chim. Hung. **129**, 719 (1992).
[13] J. Teltow, Z. Phys. Chem. B **43**, 198 (1939).
[14] L. W. Johnson and S. P. McGlynn, Chem. Phys. Lett. **7**, 618 (1970).
[15] V. A. Gubanov, J. Weber, and J. W. D. Connoly, J. Chem. Phys. **63**, 1455 (1975).
[16] R. M. Millier, D. S. Tinti, and D. A. Cose, Inorg. Chem. **28**, 2738 (1989).
[17] H. Nakatsuji and S. Saito, Int. J. Quantum Chem. **39**, 93 (1991).
[18] H. Nakatsuji and S. Saito, J. Chem. Phys. **93**, 1865 (1990).
[19] H. Nakatsuji, M. Ehara, M. H. Palmer, and M. F. Guest, J. Chem. Phys. **87**, 2561 (1992).
[20] K. Yasuda and H. Nakatsuji, J. Chem. Phys. **99**, 1945 (1993).
[21] G. V. Girichev, N. I. Giricheva, E. A. Kuligin, and K. S. Krasnov, Zh. Strukt. Khim. **24**, 1 (1983); Russ. J. Struct. Chem. (English translation) **24**, 55 (1983).
[22] S. Huzinaga, J. Andzelm, M. Klobukowski, E. Radzio-Andzelm, Y. Sakai, and H. Tatewaki, *Gaussian Basis Sets for Molecular Calculations* (Elsevier, New York, 1984).
[23] S. Huzinaga, J. Chem. Phys. **42**, 1293 (1965).
[24] T. H. Dunning, Jr., J. Chem. Phys. **53**, 2823 (1970).
[25] M. Dupuis, J. D. Watts, H. O. Viller, and G. J. B. Hurst, Program Library HONDO7 No. 1501, Computer Center of the Institute for Molecular Science, 1989.
[26] H. Nakatsuji, Program System for SAC and SAC-CI calculations, Program Library No. 146 Y4/SAC, Data Processing Center of Kyoto University, 1985; Program Library SAC85, No. 1396, Computer Center of the Institute for Molecular Science, 1986.
[27] H. Nakatsuji, Chem. Phys. **75**, 425 (1983).
[28] J. C. Duinker and C. J. Ballhausen, Theor. Chim. Acta. **12**, 325 (1968).
[29] J. P. Dahl and H. Johansen, Theor. Chim. Acta. **11**, 8 (1968).